ScientificScholar®
Knowledge is power
Publisher of Scientific Journals

www.surgicalneurologyint.com

Surgical Neurology International

Editor-in-Chief: Nancy E. Epstein, MD, Professor of Clinical Neurosurgery, School of Medicine, State U. of NY at Stony Brook.

SNI: Neuro-Oncology

Editor
Mitsutoshi Nakada, MD
Kanazawa University, Ishikawa, Japan

SNI
Open Access

Original Article

Artificial intelligence in corticospinal tract segmentation using constrained spherical deconvolution

Erom Lucas Alves Freitas[1], Bruno Fernandes de Oliveira Santos[1,2]

[1]Department of Medicine, Federal University of Sergipe, [2]Health Sciences Graduate Program, Federal University of Sergipe, Aracaju, Brazil.

E-mail: Erom Lucas Alves Freitas - eromfreitas10@gmail.com; *Bruno Fernandes de Oliveira Santos - brunofernandes.se@gmail.com

***Corresponding author:**
Bruno Fernandes de Oliveira Santos,
Health Sciences Graduate Program, Federal University of Sergipe, Aracaju, Brazil.

brunofernandes.se@gmail.com

Received: 22 November 2024
Accepted: 30 December 2024
Published: 31 January 2025

DOI
10.25259/SNI_982_2024

Quick Response Code:

ABSTRACT

Background: Tractography of cerebral white matter tracts is a technique with applications in neurosurgical planning and the diagnosis of neurological diseases. In this context, the approach based on the constrained spherical deconvolution (CSD) algorithm allows for more efficient and plausible segmentations. This study aimed to compare two CSD techniques for corticospinal tract (CST) segmentation.

Methods: This study examined 40 diffusion-weighted images (DWIs) acquired at 7T from healthy participants in the human connectome project (HCP) and 12 clinical 1.5T DWIs from patients undergoing neurosurgical procedures. Tractography was performed using two techniques: regions of interest-based approach and an automatic approach using the TractSeg neural network. The volume of the CST segmented by the two methods was compared using the Dice similarity coefficient.

Results: There was a low similarity between the CST volumes segmented by the two techniques (Dice index for the HCP: 0.479 ± 0.04; Dice index for the Clinical: 0.404 ± 0.08). However, both techniques achieved high levels of consistency in sequential measurements, with intraclass correlation coefficient values above 0.995 for all comparisons. In addition, all selected metrics showed significant differences when comparing the two techniques (HCP – volume $P < 0.0001$, fractional anisotropy [FA] $P = 0.0061$, mean diffusivity [MD] $P < 0.0001$; Clinical – volume $P < 0.0001$, FA $P = 0.0018$, MD $P = 0.0018$).

Conclusion: Both methods demonstrate a high degree of consistency; however, the automatic approach appears to be more consistent overall. When comparing the CST segmentations between the two methods, we observed only a moderate similarity and differences in all considered metrics.

Keywords: Constrained spherical deconvolution, Corticospinal tract, Tractography probabilistic, TractSeg

INTRODUCTION

The advent of tractography techniques for *in vivo* segmentation of cerebral white matter tracts has enabled greater precision in neurosurgical planning and expanded the diagnostic arsenal for neurological pathologies.[16] This technique usually utilizes diffusion tensor imaging (DTI) to gather information about the magnitude and orientation of water molecules in tissue, thereby virtually reconstructing their pathways along axonal fibers.[18,20]

Historically, classical DTI tractography faced inherent challenges, such as the issue of crossing fibers and the reconstruction of tracts following more curvilinear trajectories. In this context, the emergence and successful implementation of tractography based on the constrained spherical

deconvolution (CSD) algorithm[27] have facilitated the reconstruction of white matter tracts by overcoming the problem of crossing fibers. Such an approach offers a solution by estimating multiple fiber orientations within a single voxel, enabling more precise tractography.[15]

The corticospinal tract (CST) stands as the primary descending motor pathway usually explored by neurosurgeons and neuroradiologists.[11,21,33] Accurate mapping of the CST is vital for adequate surgical planning. However, DTI has limitations, mainly in tracking fibers originating from the lateral motor cortex, which is responsible for the facial muscles. Our goal is to achieve a more comprehensive and accurate reconstruction of the CST compared to traditional DTI methods. This new approach could enhance clinical and surgical outcomes.[11,34]

The objective of this study was to compare two CSD-based tractography methods using 40 diffusion images from the human connectome project (HCP) of healthy individuals and 12 clinical diffusion-weighted images (DWI) from patients who underwent neurosurgical procedures, with a focus on CST segmentation. The study aimed to evaluate the similarity between the two techniques and the specific consistency of their measurements.

MATERIALS AND METHODS

Image acquisition

HCP dataset

We evaluated a total of 40 DWIs from 7 Tesla magnetic resonance imaging (MRI) scans, randomly selected from anonymized healthy patients in the HCP database, comprising 29 women and 11 men aged between 22 and 35 years. The acquisition protocol for these images included a spin-echo echo-planar imaging sequence with a repetition time (TR) of 7000 ms, TE of 71.2 ms, b-values of 1000 and 2000 s/mm², and an echo spacing of 0.82 ms. Structural T1-weighted images were obtained using Siemens devices.

Clinical dataset

In addition, we selected 12 DWI datasets from patients with pathological conditions to evaluate the consistency of the two tractography techniques in challenging conditions. Among the selected scans, 10 were from patients with intracranial tumors, and two were from patients with Parkinson's disease undergoing deep brain stimulation (DBS). This cohort included eight women and four men aged between 6 and 69 years. The cranial MRI images were obtained using a SIGNA Explorer 1.5T scanner (GE Healthcare, Chicago, Illinois, USA), with the following technical specifications: a gradient strength of 40 mT/m, a matrix of 256 × 256 pixels, a field of view of 256 × 256 mm, and a slice thickness of 1 mm. The DWI sequences were acquired in the axial plane with a TR of 8.23 ms and time to echo (TE) of 0.1057 s, using 32 directions. The T1-weighted sequences were acquired in the sagittal plane with a TR of 0.008516 s and TE of 0.003492s.

Inclusion and exclusion criteria for HCP and Clinical data

Inclusion criteria were MRI scans, including anatomical (T1-weighted) images and DTI. Exclusion criteria were poor-quality DWIs or the absence of any required images for processing.

Preprocessing

HCP group

The HCP DWI data had already undergone motion distortion correction using the top-up method and correction for distortions induced by eddy currents; thus, no additional preprocessing steps were necessary.[6]

Clinical group

The diffusion images of patients selected for this study were subjected to preprocessing steps due to their acquisition in a clinical context. Initially, the tool *dwidenoise*[29] was used to remove signal noise, and the tool *mrdegibbs*[12] was employed to eliminate Gibbs artifacts in the DWIs. In addition, the method *dwifslpreproc* was applied to all twelve DWIs for correcting distortions due to susceptibility effects.[2]

CSD tractography

CSD is a technique that refines another signal-processing method called spherical deconvolution. This method involves recovering a signal based on the convolution of an expected response with a known function.[27] The mathematical basis of CSD is to estimate the fiber orientation distribution (FOD) in each voxel from the diffusion signal.[27] The FOD represents the spatial arrangement of fibers within each voxel, while the FOD function (fODF) mathematically describes this distribution.[25,26]

Preprocessing for CSD tractography

The next step was to estimate the response function using *dwi2response* with the Tournier algorithm [25], which selects a single fiber per voxel. Subsequently, the fODF was estimated using *dwi2fod,*[27] enabling tractography capable of tracking within complex neuroanatomy, making the process more robust and reliable.

Definition of ROIs

We used the MRtrix3 software package to perform segmentation based on regions of interest (ROIs) defined by

atlases. For segmenting the CST, we based our approach on defining cortical and subcortical regions to delineate fiber tracking. Specifically, we selected the precentral gyrus as defined by the Juelich Cytoarchitectonic Atlas,[1] designating it as the initial region for processing.

The Johns Hopkins University International Consortium for Brain Mapping DTI-81 Atlas (JHU-ICBM-DTI-81)[8] was used to define the ROI corresponding to the posterior limb of the internal capsule (PLIC), considered an inclusion region. In addition, the Harvard-Oxford Structural Atlas defined an inclusion ROI corresponding to the brainstem.[14] Finally, as defined by the JHU-ICBM-DTI-81, the corpus callosum was used as an exclusion region to prevent tracking fibers into the contralateral hemisphere.

The ROIs were registered to each subject's native diffusion space using diffeomorphic nonlinear co-registration with the assistance of advanced normalization tools (ANTs) software.[3]

Atlas-based tractography

The probabilistic tractography algorithm chosen was second-order integration over fiber orientation distributions (iFOD2), configured in the *tckgen* tool of MRtrix3.[4] We specified the PLIC as the seed region and the origin of fiber propagation and selected the precentral gyrus and brainstem as inclusion regions, excluding all fibers directed toward the corpus callosum. We also set a maximum of 5,000 streamlines, terminating the tracking once this number was reached. The CST was segmented twice sequentially in all individuals to allow for test-retest analysis.

Subsequently, all generated segmentations were registered to the common space of the Montreal Neurological Institute (MNI) fractional anisotropy (FA) map using the functional magnetic resonance imaging of the brain (FMRIB) Software Library[9] and the FMRIB Linear Image Registration Tool and the transformation was applied using MRtrix3 *tcktransform.*[28] This step was performed to enable comparison between subjects.

TractSeg

TractSeg is a tractography tool based on a pretrained convolutional neural network model that automatically segments up to 72 predefined white matter tracts.[30,31] Since the tool was developed using diffusion images from HCP patients, no additional preprocessing was performed on the selected patient group for this study, as suggested by the official documentation. Conversely, all 12 DWIs from the group of pathological individuals underwent the preprocessing steps described above (noise removal, artifact correction, and motion correction), allowing us to perform tractography through TractSeg on these images.

According to the documentation protocol, all diffusion images are aligned to the common MNI space[5] through the FA image, enhancing processing stability and enabling subsequent comparative analyses between individuals. For this study, we selected only the CST tract and limited tracking to 5,000 streamlines, using the CSD algorithm for fODF estimation. All other TractSeg settings were kept as default. In all individuals, the segmentation was performed twice sequentially.

In the clinical group, for cases of intracranial tumors, the accuracy of the tractography was intraoperatively evaluated through motor mapping with direct stimulation of the motor area (cortical) and motor fibers (subcortical). The Eximius Med neuronavigation platform (Artis, Brasilia, Brazil) was used for this purpose. The nerve monitoring systems (NIM) Eclipse 32-channel system from Medtronic (Medtronic, Dublin, Ireland) was used in conjunction with the platform Eximius MED. The procedures were performed for DBS cases using stereotaxy Invoked ZD Arc and microstimulation (Inomed Medizintechnik GmbH, Emmendingen, Germany) associated with Eximius Med Software Stereotactic Module (Artis, Brasilia, Brazil).

Metrics

We evaluated the similarity of CST segmentations using MRtrix3 and TractSeg through the Dice-Sørensen coefficient (DICE Index).[24] The calculation is done using the formula: DICE = 2TP/(2TP + FP + FN), where true positive (TP), false positive (FP), and false negative (FN).

In addition, we selected three metrics for the quantitative evaluation of the tracts: the volume of the density map for each segmentation, the mean FA value, and the mean diffusivity (MD) value along the tract.[13] FA and MD values were obtained using *dtifit*, which fits a diffusion tensor model at each voxel. Subsequently, we used the *tckmap* tool to map the corresponding values to the segmented CST from the tensor images.[4]

Finally, we extracted the mean values of the metrics for each segmented CST from the patients using the *mrstats* tool.[28] For volume, we used the *fslstats* tool to extract the mean volume of the CST segmentation in each voxel for each technique.[10]

Statistical analysis

We used the DICE Index to evaluate the overlap in CST volume generated by the two techniques. In addition, we performed a consistency analysis of the sequential measurements using the intraclass correlation coefficient (ICC) with a two-way random model. The metrics extracted from each technique were subjected to a Shapiro–Wilk normality test. Continuous variables were compared using the *t*-test or Wilcoxon test, as appropriate, with a significance level of $P < 0.05$. Analysis was performed using R statistical

Table 1: Demographic characteristics of participants in the clinical group.

Index	Sex	Disease	Age	Confirmation in Neuromonitoring	Neuromonitoring
Case 1	Masculine	Tumor	54	Y	Intact
Case 2	Masculine	Tumor	29	Y	Grade V muscle weakness progressed to right hemiparesis and grade IV muscle strength
Case 3	Feminine	Tumor	58	N	Intact
Case 4	Masculine	Tumor	30	Y	Previous deficit maintained
Case 5	Feminine	Parkinson's disease - STN DBS	69	Y	Intact
Case 6	Feminine	Tumor	59	Y	Intact
Case 7	Feminine	Tumor	66	Y	Previous deficit maintained
Case 8	Feminine	Tumor	69	Y	Intact
Case 9	Feminine	Tumor	51	Y	Previous deficit maintained
Case 10	Masculine	Parkinson's disease - STN DBS	65	Y	Intact
Case 11	Feminine	Tumor	27	Y	Intact
Case 12	Feminine	Tumor	6	Y	Intact

Y: Yes; N: No; STN DBS: Subthalamic nucleus deep brain stimulation

Table 2: Dice index of the corticospinal tract from consecutive measurements and comparison between techniques.

TractSeg		Atlas-based	TractSeg x Atlas-based	*p*-value
HCP	0.895 (±0.01)	0.893 (±0.01)	0.479 (±0.04)	0.5333
Clinical	0.887 (±0.01)	0.810 (±0.04)	0.404 (±0.08)	0.0001
P-value	0.11	<0.0001		

HCP Human Connectome Project
Welch's t-test comparing HCP x Clinical
Paired t-test comparing TractSeg x Atlas-based

Table 3: Consistency analysis using the Intraclass Correlation Coefficient of two consecutive measurements of the corticospinal tract tractography metrics.

Test x Retest	Volume	FA	MD (x10-4)
HCP - Tractseg	0.998	0.999	0.999
HCP - Atlas-based	0.999	0.998	0.995
Clinical - Tractseg	0.998	1	1
Clinical - Atlas-based	0.999	0.998	0.995

HCP Human Connectome Project
FA: Fractional anisotropy, MD: Mean diffusivity
$P<0.05$

software (version 4.3.2) and the PyCharm development environment (March 03, 2023) with Python (version 3.10).

Ethics aspects

The images from the HCP database used in this research are public domain and do not require permission for data use. For the clinical group images, all patients provided informed consent for the use of the images, and all data were anonymized to ensure data privacy. This research was submitted to and approved by the Ethics and Research Committee of the Federal University of Sergipe under process number 6.836.579.

RESULTS

In the clinical group, the mean age was 44.9 years (interquartile range 29.5) for those undergoing brain tumor resection [Table 1]. Table 2 shows the DICE index values for the similarity of the CST segmented volumes using TractSeg and the atlas-based approach. Regarding the similarity of the segmented volumes, there was moderate similarity between the results generated by the two techniques evaluated for both the HCP (0.479 ± 0.04) and clinical groups (0.404 ± 0.08).

When comparing the consistency of the two methods (atlas-based and TractSeg) using the DICE index, they are comparable in the HCP group. However, in clinical cases, the automatic method (TractSeg) demonstrates superior consistency compared to the atlas-based method (0.89 ± 0.01 vs. 0.81 ± 0.04, $P < 0.001$). Furthermore, TractSeg maintains high consistency regardless of the sample considered (HCP or clinical). In contrast, the consistency of the atlas-based method is significantly influenced by the type of sample ($P < 0.001$).

The consistency analysis of the two techniques (atlas-based and TractSeg) across consecutive measurements (test-retest) of CST volume, FA, and MD are shown in Table 3. Both techniques demonstrated a high degree of consistency in terms of tract volume, FA, and MD metrics, as assessed by the ICC in both the HCP and clinical groups.

Comparisons between the automatic and atlas-based approaches showed significant differences in volume for both the HCP ($P < 0.0001$) and clinical ($P < 0.0001$) groups [Table 4]. Similarly, significant differences were observed in the mean FA metric values between the two approaches in the HCP (Wilcoxon, $P = 0.0061$) and clinical (Wilcoxon, $P = 0.0018$) groups. Furthermore, the MD metric also exhibited significant differences between the automatic and atlas-based approaches in both groups (HCP: $P < 0.0001$; clinical: $P = 0.0018$).

The three-dimensional projection of the CST using TractSeg and MRtrix, focusing on the HCP individual with the highest DICE index (0.551), is shown in Figure 1. Similarly, Figure 2 illustrates the CST segmentation in several images of pathological patients, highlighting the relationship between the tract and the adjacent tumor lesion.

In participants who underwent neurosurgical intervention, the segmentation results obtained through TractSeg were consistent with intraoperative monitoring findings. In these cases, the generated tracts, when associated with neuronavigation, aligned with the results of neurophysiological monitoring. Intraoperative neuromonitoring, when available, confirmed the tract localization in the precise location indicated by the tractography in all cases. Only one case was operated on without intraoperative neuromonitoring, making it impossible to confirm the tract localization for that particular case.

DISCUSSION

In this study, we reconstructed the CST using two CSD-based tractography techniques and evaluated the similarity and consistency of the generated segmentations. Our findings demonstrate a high similarity of the CST generated consecutively within each technique, suggesting that both methods produce consistent results. However, the automatic approach appears to be more consistent overall. When comparing the CST segmentations between the two methods, we observed a moderate similarity. Importantly, in terms of clinical relevance, the automatic approach showed consistency with intraoperative findings, validating its potential for surgical planning and guidance.[22,23,30]

Our findings indicate significant differences between the two CSD tractography techniques studied. However, it is noteworthy that both techniques demonstrated high consistency in consecutive segmentations, indicating that,

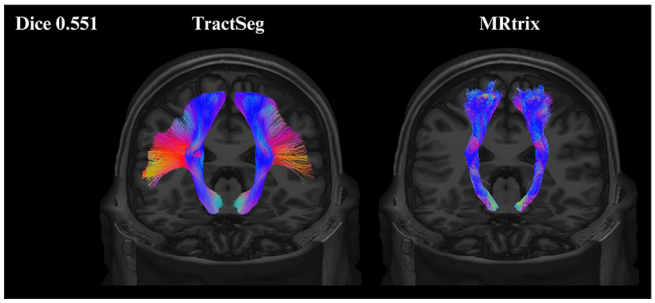

Figure 1: Three-dimensional representation of the best and worst overlap of the corticospinal tract volume segmented by the two techniques evaluated in human connectome project individuals.

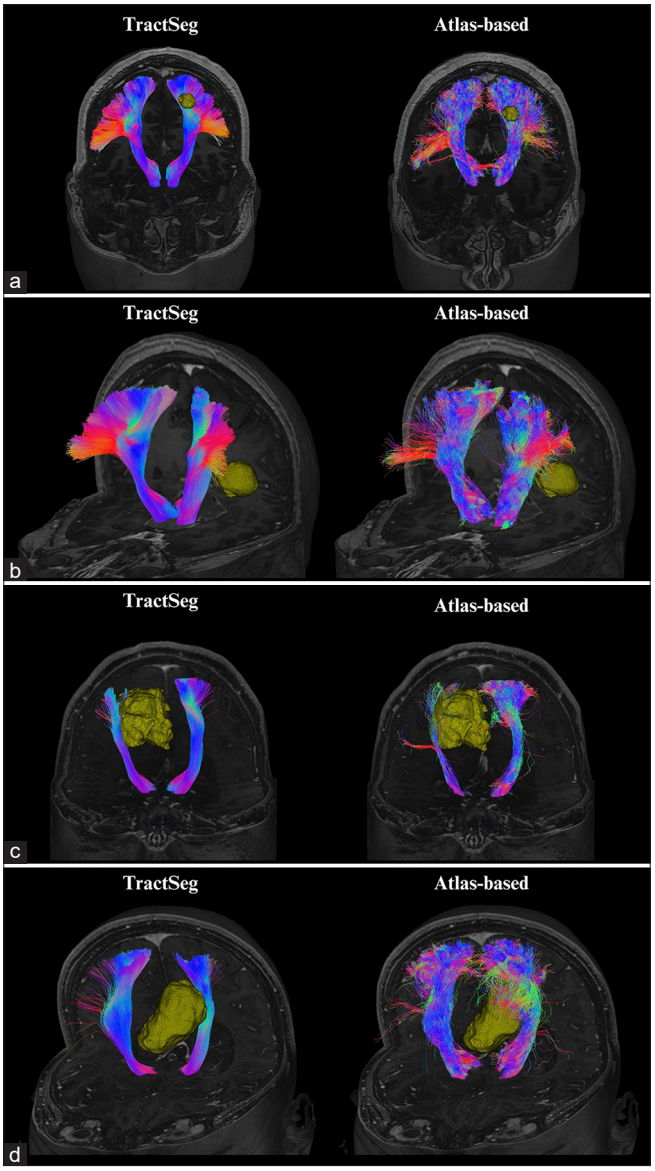

Figure 2: Three-dimensional projection of the corticospinal tract segmentation using the two chosen techniques on clinical T1 images. (a) Corticospinal Tract Segmented through the techniques evaluated in anterior view; (b) corticospinal tract segmented by techniques evaluated in left oblique view; (c) corticospinal Tract Segmented through the techniques evaluated in anterior view; (d) corticospinal tract segmented by techniques evaluated in oblique and left superior view.

Table 4: Tractographic metrics of the corticospinal tract via TractSeg and atlas-based method.

	Volume	FA	MD (x10-4)
HCP – TractSeg	45,858 (±4,163)	0.4673 (±0.0162)	4.927 (±0.105)
HCP - Atlas-based	37,365 (±5,867)	0.4535 (±0.0239)	5.117 (±0.128)
p-value	< 0.0001	0.0061	< 0.0001
Clinical - TractSeg	32,007 (±8,949)	0.4416 (±0.4930)	8.499 (±0.642)
Clinical - Atlas-based	79,926 (±22,152)	0.3630 (±0.0522)	9.685 (±0.981)
p-value	< 0.0001	0.0018	0.0018

HCP Human Connectome Project
FA: Fractional anisotropy, MD: Mean diffusivity
Wilcoxon test for metrics considering TractSeg vs. MRtrix

although they produce different results, they are robust in the reproducibility of their outcomes.

In the HCP group, which has a more homogeneous anatomy, the volume generated by TractSeg was more significant than that generated by MRtrix, and this relationship was reversed when segmenting the CST in clinical images with significant structural differences. This paradoxical result may indicate that in the presence of topographical heterogeneity, the automatic approach is more refined and accounts for structural alterations. In contrast, the atlas-based approach is more susceptible to false positives, characterized by the continuation of fiber tracking even when physically impossible.[7,19]

Considering the HCP group, the difference in CST generated by each technique is evident, with TractSeg showing better delineation of fibers according to their cortical arrangement. The automatic segmentation better represented curvilinear fibers. In the clinical group, the presence of tumor masses posed a significant challenge for both techniques, and it was clear, as shown in Figure 2, that TractSeg better-tracked fibers, considering the anatomical alterations imposed by the tumor.

In the noteworthy case presented in Figure 2, the atlas-based technique traced more fibers than the automatic one (TractSeg), despite the presence of a large tumor mass altering the brain architecture. This significant difference can be attributed to the greater susceptibility of the atlas-based approach to false positives, which may limit its reliability in guiding surgical interventions, particularly in the presence of brain tumors. Automatic techniques offer a promising alternative for obtaining more accurate and patient-specific CST reconstructions, which may ultimately lead to improved surgical outcomes and reduced postoperative motor deficits.[16]

In patients undergoing neurosurgery, the locations of tracts generated through TractSeg and neuronavigation were consistent with observations in neurophysiological monitoring. Thus, TractSeg is reliable and robust, not only for its high reproducibility but also for its accuracy in neurosurgical applications.[16] This applies to both tumor resections closely associated with eloquent areas and assisting electrode placement in DBS surgeries.

Our findings point to the superiority of the automatic tractography method through TractSeg compared to the widely used atlas-based approach, which has limitations that compromise its results. In this sense, the automatic segmentation of cerebral white matter tracts, including the CST, represents the state-of-the-art technique in tractography.[11]

This represents a significant advance for tractography applications in neurosurgical planning and clinical diagnosis of neurological diseases affecting white matter.[32,33] In addition, intraoperative neurophysiological monitoring to confirm the CST location indicated by TractSeg highlights the safety of using this technique, enabling its use in clinical-surgical contexts.

Limitations

The most crucial limitation concerns the implementation of TractSeg, as it is still less common than other approaches and requires programming language knowledge, which can pose execution obstacles. In addition, atlas-assisted ROI demarcation has limitations compared to manual demarcation when considering specific neuroanatomical characteristics.[17] Regarding CSD-based tractography, another limitation is the difficulty of finding effects in small samples.[34]

The limitation of the clinical image dataset size, although significant, was mitigated by employing robust statistical data analysis techniques aimed at extracting relevant and reliable information.

CONCLUSION

Both methods demonstrate a high degree of consistency; however, the automatic approach appears to be more

consistent overall. When comparing the CST segmentations between the two methods, we observed only a moderate similarity and differences in all considered metrics (CST volume, FA, and MD).

Ethical approval: The research/study was approved by the Institutional Review Board at the Ethics and Research Committee of the Federal University of Sergipe, number 6.836.579, dated May 21, 2024.

Declaration of patient consent: The authors certify that they have obtained all appropriate patient consent.

Financial support and sponsorship: Nil.

Conflicts of interest: There are no conflicts of interest.

Use of artificial intelligence (AI)-assisted technology for manuscript preparation: The authors confirm that there was no use of artificial intelligence (AI)-assisted technology for assisting in the writing or editing of the manuscript and no images were manipulated using AI.

REFERENCES

1. Amunts K, Mohlberg H, Bludau S, Zilles K. Julich-brain: A 3D probabilistic atlas of the human brain's cytoarchitecture. Science 2020;369:988-92.
2. Andersson JL, Sotiropoulos SN. An integrated approach to correction for off-resonance effects and subject movement in diffusion MR imaging. Neuroimage 2016;125:1063-78.
3. Avants BB, Tustison NJ, Song G, Cook PA, Klein A, Gee JC. A reproducible evaluation of ANTs similarity metric performance in brain image registration. Neuroimage 2011;54:2033-44.
4. Calamante F, Tournier JD, Heidemann RM, Anwander A, Jackson GD, Connelly A. Track density imaging (TDI): validation of super resolution property. Neuroimage 2011;56:1259-66.
5. Fonov V, Evans A, McKinstry R, Almli C, Collins D. Unbiased nonlinear average age-appropriate brain templates from birth to adulthood. Neuroimage 2009;47:S102.
6. Glasser MF, Smith SM, Marcus DS, Andersson JL, Auerbach EJ, Behrens TE, *et al.* The Human Connectome Project's neuroimaging approach. Nat Neurosci 2016;19:1175-87.
7. Gutierrez CE, Skibbe H, Nakae K, Tsukada H, Lienard J, Watakabe A, *et al.* Optimization and validation of diffusion MRI-based fiber tracking with neural tracer data as a reference. Sci Rep 2020;10:21285.
8. Hua K, Zhang J, Wakana S, Jiang H, Li X, Reich DS, *et al.* Tract probability maps in stereotaxic spaces: Analyses of white matter anatomy and tract-specific quantification. Neuroimage 2008;39:336-47.
9. Jenkinson M, Bannister P, Brady M, Smith S. Improved optimization for the robust and accurate linear registration and motion correction of brain images. Neuroimage 2002;17:825-41.
10. Jenkinson M, Beckmann CF, Behrens TE, Woolrich MW, Smith SM. FSL. Neuroimage 2012;62:782-90.
11. Kamagata K, Andica C, Uchida W, Takabayashi K, Saito Y, Lukies M, *et al.* Advancements in diffusion MRI tractography for neurosurgery. Invest Radiol 2024;59:13-25.
12. Kellner E, Dhital B, Kiselev VG, Reisert M. Gibbs-ringing artifact removal based on local subvoxel-shifts. Magn Reson Med 2016;76:1574-81.
13. Luque Laguna PA, Combes AJ, Streffer J, Einstein S, Timmers M, Williams SC, *et al.* Reproducibility, reliability and variability of FA and MD in the older healthy population: A test-retest multiparametric analysis. NeuroImage Clin 2020;26:102168.
14. Makris N, Goldstein JM, Kennedy D, Hodge SM, Caviness VS, Faraone SV, *et al.* Decreased volume of left and total anterior insular lobule in schizophrenia. Schizophr Res 2006;83:155-71.
15. Mormina E, Longo M, Arrigo A, Alafaci C, Tomasello F, Calamuneri A, *et al.* MRI tractography of corticospinal tract and arcuate fasciculus in high-grade gliomas performed by constrained spherical deconvolution: Qualitative and quantitative analysis. Am J Neuroradiol 2015;36:1853-8.
16. Moshe YH, Ben Bashat D, Hananis Z, Teicher M, Artzi M. Utilizing the TractSeg tool for automatic corticospinal tract segmentation in patients with brain pathology. Technol Cancer Res Treat 2022;21:15330338221131387.
17. O'Donnell LJ, Suter Y, Rigolo L, Kahali P, Zhang F, Norton I, *et al.* Automated white matter fiber tract identification in patients with brain tumors. NeuroImage Clin 2017;13:138-53.
18. Panesar SS, Abhinav K, Yeh FC, Jacquesson T, Collins M, Fernandez-Miranda J. Tractography for surgical neuro-oncology planning: Towards a gold standard. Neurotherapeutics 2019;16:36-51.
19. Petersen MV, McIntyre CC. Comparison of anatomical pathway models with tractography estimates of the pallidothalamic, cerebellothalamic, and corticospinal tracts. Brain Connect 2023;13:237-46.
20. Pujol S, Wells W, Pierpaoli C, Brun C, Gee J, Cheng G, *et al.* The DTI challenge: Toward standardized evaluation of diffusion tensor imaging tractography for neurosurgery. J Neuroimaging 2015;25:875-82.
21. Rheault F, De Benedictis A, Daducci A, Maffei C, Tax CM, Romascano D, *et al.* Tractostorm: The what, why, and how of tractography dissection reproducibility. Hum Brain Mapp 2020;41:1859-74.
22. Richards TJ, Anderson KL, Anderson JS. Fully automated segmentation of the corticospinal tract using the TractSeg algorithm in patients with brain tumors. Clin Neurol Neurosurg 2021;210:107001.
23. Simon HA. Artificial intelligence: Where has it been, and where is it going? IEEE Trans Knowl Data Eng 1991;3:128-36.
24. Taha AA, Hanbury A. Metrics for evaluating 3D medical image segmentation: Analysis, selection, and tool. BMC Med Imaging 2015;15:29.
25. Tournier JD, Calamante F, Connelly A. Determination of the appropriate b value and number of gradient directions for high-angular-resolution diffusion-weighted imaging. NMR Biomed 2013;26:1775-86.
26. Tournier JD, Calamante F, Connelly A. MRtrix: Diffusion tractography in crossing fiber regions. Int J Imaging Syst Technol 2012;22:53-66.
27. Tournier JD, Calamante F, Connelly A. Robust determination of the fibre orientation distribution in diffusion MRI: Non-negativity constrained super-resolved spherical deconvolution. Neuroimage 2007;35:1459-72.

28. Tournier JD, Smith R, Raffelt D, Tabbara R, Dhollander T, Pietsch M, *et al.* MRtrix3: A fast, flexible and open software framework for medical image processing and visualisation. Neuroimage 2019;202:116137.
29. Veraart J, Novikov DS, Christiaens D, Ades-Aron B, Sijbers J, Fieremans E. Denoising of diffusion MRI using random matrix theory. Neuroimage 2016;142:394-406.
30. Wasserthal J, Maier-Hein KH, Neher PF, Northoff G, Kubera KM, Fritze S, *et al.* Multiparametric mapping of white matter microstructure in catatonia. Neuropsychopharmacology 2020;45:1750-7.
31. Wasserthal J, Neher P, Maier-Hein KH. TractSeg - Fast and accurate white matter tract segmentation. Neuroimage 2018;183:239-53.
32. Wasserthal J, Neher PF, Hirjak D, Maier-Hein KH. Combined tract segmentation and orientation mapping for bundle-specific tractography. Med Image Anal 2019;58:101559.
33. Young F, Aquilina K, Seunarine KK, Mancini L, Clark CA, Clayden JD. Fibre orientation atlas guided rapid segmentation of white matter tracts. Hum Brain Mapp 2024;45:e26578.
34. Zhylka A, Sollmann N, Kofler F, Radwan A, De Luca A, Gempt J, *et al.* Reconstruction of the corticospinal tract in patients with motor-eloquent high-grade gliomas using multilevel fiber tractography combined with functional motor cortex mapping. Am J Neuroradiol 2023;44:283-90.

How to cite this article: Freitas EL, Fernandes de Oliveira Santos B. Artificial intelligence in corticospinal tract segmentation using constrained spherical deconvolution. Surg Neurol Int. 2025;16:32. doi: 10.25259/SNI_982_2024